Synthesis and Characterization of Polyaniline/Graphite Composites and Study of Their Electrical and Electrochemical Properties

S. Konwer, B. Pokhrel, S. K. Dolui

Department of Chemical Sciences, Tezpur University, Napaam, Assam 784028, India

Received 22 April 2009; accepted 21 October 2009
DOI 10.1002/app.31633
Published online 17 December 2009 in Wiley InterScience (www.interscience.wiley.com).

ABSTRACT: Polyaniline/graphite (PA/G) composites were prepared by the incorporation of graphite in various proportions (0.2, 0.5, and 1.0%) into polyaniline (PA) through the *in situ* polymerization of aniline. The polymer composites were characterized by Fourier transform infrared (FTIR) spectroscopy, ultraviolet–visible (UV–vis) spectroscopy, X-ray diffraction, scanning electron microscopy, thermogravimetric analysis, differential scanning calorimetry, a four-probe method, current–voltage characteristics, and cyclic voltammetry (CV). FTIR and UV–vis spectroscopy revealed interaction between graphite and the imine groups of PA. The polymer composites showed a crystalline nature with a hexagonal primitive structure. The uniform distribution of graphite particles was observed within the polymer matrix. The composites were found to possess good thermal stability up to 573 K. The conductivity of the composites was in the range 4.53–238.08 S/cm, and the conductivity varied with temperature. The band gap of the composites was found in the range 1.2–1.6 eV. The PA/G composites also displayed a reversible electrochemical response, as revealed by the CV study. © 2009 Wiley Periodicals, Inc. J Appl Polym Sci 116: 1138–1145, 2010

Key words: adsorption; conducting polymers; fillers; synthesis; UV–vis spectroscopy

INTRODUCTION

In recent years, considerable interest has been shown in polyaniline (PA) as a conducting organic polymer because of its potential applications in new technologies, such as chemical sensors,[1,3] electrochromic displays,[4] electronic devices,[5] and secondary batteries.[6–8] PA undergoes variation in electrical conductivity by several orders of magnitude subsequent to doping. Various dopants, namely, HCl,[9] methyl sulfonic acid,[10,11] toluene sulfonic acid, sulfosalicylic acid, dodecylbenzenesulfonic acid,[12] perchloric acid,[13] and iodine,[14] have been used with PA to improve its electrical properties and chemical stability. The doping of metallic ions or particles into PA was carried out to introduce magneto conductivity properties.[15]

Doping has significantly enhanced the conductivity but has not improved the chemical stability and mechanical strength of PA. PA composite materials prepared by the incorporation of inorganic fillers, such as TiO_2, $BaTiO_3$, Mo_2S_3, V_2O_5, and fly ash,[16–20] have shown increases in conductivity, and the conductivity has increased with the content of inorganic filler. This was due to enhanced connectivity between the grains of PA particles. In addition to conductivity, the magnetic susceptibility[21] and spin dynamic properties[22] of the polymer were also improved. Many of these materials are not suitable for electrodes because of the dearth of porosity and, hence, the lesser contact area for the electrolyte.

Graphite has been used as a filler for PA to improve its chemical stability and thermal stability and to enhance the conductivity of the polymer.[23–26] There are many advantages to using graphite in composite materials, such as very good conductivity, facilitated surface polymerization,[27] better adsorption capabilities compared to other dopants, cost effectiveness, and availability in large quantities;[28] thereby, polyaniline/graphite (PA/G) composites would be suitable for designing high-current density galvanic cells.[29] Different sizes of graphite particles were incorporated into the PA matrix to form a PA/G composite only by electrochemical polymerization.[30] The graphite particles were modified with hydroxyl, carbonyl, and ether group functionalities.[31]

In this article, we discuss the preparation of PA/G composites with graphite contents varying from 0.2 to 1.0% (w/v) by the *in situ* polymerization of aniline. *In situ* chemical methods offer an advantage over methods involving the chemical polymerization

Correspondence to: S. K. Dolui (dolui@tezu.ernet.in).
Contract grant sponsor: Board of Research in Nuclear Sciences (BRNS), Department of Atomic Energy (DAE), India; contract grant number: 2008/37/37/BRNS/2470.

of the monomer in the sense that the composites are obtained in the powder form, whereas a composite film is obtained in electropolymerization. Also, there is some possibility of incorporating graphite into the main chain of the polymer. The main disadvantages of electropolymerization are a low conductivity and a low yield percentage of polymer product compare to chemical polymerization.[32] Because of the high conductivity, this is especially important in some applications, including batteries,[6] sensors,[3] and electronic devices.[5]

Thus, in this study, we chemically synthesized PA/G composites and evaluated their concomitant properties, namely, the electrochemical behavior, thermal behavior, surface morphology, and electrical conductivity in detail, with special emphasis on the electrical properties.

EXPERIMENTAL

Materials

Aniline and pure graphite (20 μm) were obtained from Aldrich Co. (Steinheim, Germany) and were used without further purification. Hydrochloric acid and potassium persulfate ($K_2S_2O_8$) were analytical-reagent-grade chemicals (Merck, Darmstadt, Germany) and were used as received. For all purposes, double-distilled water was used. Acetonitrile and *N*-methyl pyrrolidone were purified by standard methods.

Preparation of PA

A three-necked, round-bottom flask (250 mL) was equipped with a thermometer, a nitrogen inlet, and a dropping funnel. Aniline (0.1 mol) was dissolved in 50 mL of a 1*M* aqueous solution of HCl. The solution was cooled (273–278 K) in a salt/ice mixture. An aqueous solution of 25 mL (0.125 mol) of potassium persulfate was placed in a dropping funnel and added very slowly to the aniline solution while the temperature was maintained in a range close to 273–278 K with vigorous stirring for 2 h. The monomer-to-initiator molar ratio was maintained at 4 : 5 for the standard preparation of PA.[33] The reaction mixture was then allowed to stir at room temperature (300 K) for another 2 h. The solid precipitate of PA–HCl salt was first collected from the reaction mixture by filtration and washed thoroughly with 1*M* HCl and then distilled water and 250 mL of ethanol. The filtrate was dried at room temperature *in vacuo*.

Preparation of the PA/G composites

PA/G composites were synthesized by an *in situ* polymerization technique. In a 250-mL, three-necked flask, 0.10 mol of aniline was dissolved in 50 mL of 0.1*M* HCl, and different concentrations (0.2, 0.5, and 1.0% w/v of aniline) of graphite powder were dispersed in the aniline solutions. The initial polymerization reaction was carried out at 273–278 K for 2 h, and the further polymerization was carried out at room temperature (300 K) for another 2 h. The precipitates of the PA/G composites were first washed with 0.1*M* HCl and then by distilled water and 250 mL of ethanol. The polymer composites were finally dried *in vacuo*.

Characterization of the products

Fourier transform infrared (FTIR) spectroscopy

The IR spectra of the composites were recorded on a Nicolet Impact-410 IR spectrometer (USA) in KBr medium at room temperature in the region 4000–450 cm^{-1}.

Ultraviolet–visible (UV–vis) spectroscopy

The UV–vis absorption spectra of the samples in 1-methyl-2-pyrrolidone solvent were recorded in the range 300–800 nm with a Shimadzu UV-2550 UV–vis spectrophotometer (Japan).

X-ray diffraction (XRD)

Powder XRD data were collected on a Rigaku Miniflex X-ray diffractometer (Tokyo, Japan) with Cu Kα radiation ($\lambda = 0.15418$ nm) at 30 kV and 15 mA with a scanning rate of 0.05°/s in a 2θ range from 10 to 70°. The powder morphologies of the PA and PA/G composite were investigated with a Philips XL-30 ESEM scanning electron microscope (Tokyo, Japan).

Electrical conductivity

Pellets of the composite samples were made with a compression-molding machine with hydraulic pressure. High pressure was applied (1.5–2 ton) to the sample to get hard, round pellets (diameter = 1.5 cm, breadth = 2 mm); these pellets were used to measure the conductivity.

The electrical conductivity of the PA and PA/G composites were measured with a four-probe technique in the temperature range 300 K $\leq T \leq$ 433 K. The current–voltage (*I–V*) characteristics were studied with a Keithley 2400 source meter (USA) at room temperature in the frequency range 102–106 Hz. Voltage was applied to measure the current through the sample. The conductivity of the composite was calculated with following equation:

$$\rho = (V/I)2\pi S, \quad (1)$$

where ρ is the resistivity of the sample, V is the applied voltage, I is the measured current through the sample, and S is the distance between probes.

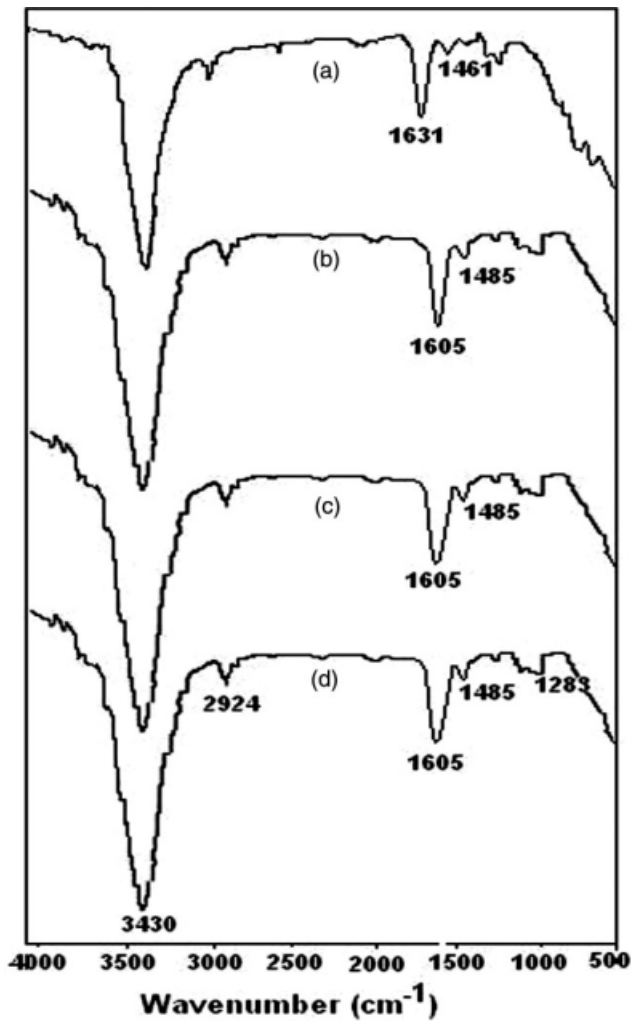

Figure 1 FTIR spectra of (a) PA, (b) PA/G (0.2%), (c) PA/G (0.5%), and (d) PA/G (1.0%).

Cyclic voltammetry (CV)

Electrochemical measurement was performed on a Sycopel AEW2-10 electrochemical work station (UK) with an Ag/AgCl reference electrode, a platinum wire as a counter electrode, and the PA/G films (0.2, 0.5, and 1.0%) on indium tin oxide (ITO) coated glass as a working electrode. The electrochemical characteristics of the polymer solution in *N*-methylpyrrolidone (NMP) were investigated by CV scanning in 0.1*M* hydrogen chloride (HCl) in acetonitrile at a scan rate of 50 mV/s.

RESULTS AND DISCUSSION

Characterization of the PA and PA/G composite

The PA/G composites were synthesized by *in situ* oxidative polymerization techniques. The aniline–hydrochloride solution may have been adsorbed on the surface of the dispersed graphite particles. This adsorbed aniline–hydrochloride on the graphite and the remaining free aniline got polymerized in the presence of the oxidizing agent to yield the PA/G composite.

The synthesized PA was in the form of an emeraldine base, as suggested from the IR data.[34] The FTIR spectrum of the synthesized PA gave absorption bands at 3430, 2924, 1631, 1461, and 1283 cm^{-1} (Fig. 1). Here, the broad absorption band at 3430 cm^{-1} indicated the secondary amine in the polymer backbone, whereas the band at 2924 cm^{-1} was due to the stretching of the C—H bonds in phenyl rings. The absorption band at 1631 cm^{-1} was obtained for the benzenoid ring, and that at 1461 cm^{-1} was for the quinoid rings. The presence of C—N—C bonds was confirmed by the absorption band at 1283 cm^{-1}.

In the PA/G composites, the absorption peaks were similar to PA, except that the absorption bands assigned to benzenoid and quinoid rings at 1631 and 1461 cm^{-1} for PA shifted to 1605 and 1485 cm^{-1} for the PA/G composites. This indicated interaction between the π-conjugated structure of the benzenoid and quinoid rings with graphite. The probable reaction of the PA/G composite is shown in Scheme 1.

Figure 2 displays the UV–vis spectra obtained from PA, the PA/G composites, and pure graphite. The spectra showed three distinct absorption bands

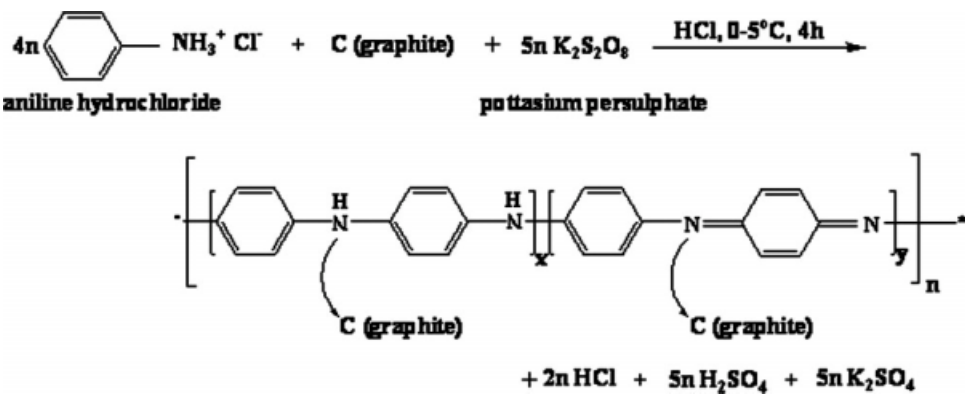

Scheme 1 *In situ* polymerization of aniline with graphite.

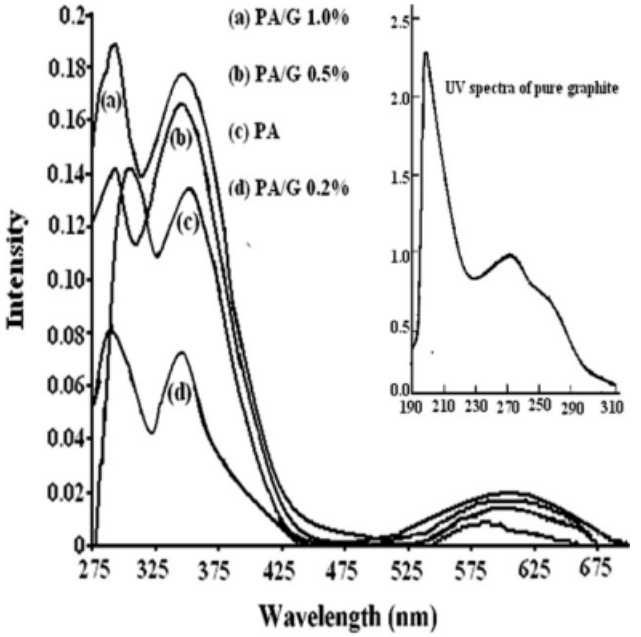

Figure 2 UV–vis spectra of (a) PA/G (1.0%), (b) PA/G (0.5%), (c) PA, and (d) PA/G (0.2%).

at 305, 356, and 630 nm for PA. The absorption band at about 305 nm was due to the excitation of nitrogen in the benzenoid and quinoid segments (π–π* transition), whereas the second and third absorption bands should have been due to the polaron transitions.[35] In the PA/G composite, the incorporated graphite interacted with the nitrogen in the benzenoid and the quinoid segments (π–π* transition); this, thereby, resulted in the shift of the band at 305.5 to 290 nm.[36] However, with the other two bands, there seemed to be no effect of incorporating graphite particles into the PA matrix. This implied that both the PA and PA/G composite showed the polaron transitions.

XRD analysis

Figure 3(a) presents the XRD pattern of pure PA, which had a broad peak at about $2\theta = 25.8^\circ$, a characteristic peak of amorphous PA. Figure 3(b–e) shows the XRD pattern of pure graphite and the PA/G composites; corresponding peaks were observed at 26.6, 44.6, and 54.85°, respectively; these peaks matched the (002), (101), and (004) planes of the hexagonal system with primitive structure (reference number PCPDFWIN 25-0284). This indicated the presence of graphite in the PA/G composites. The *d*-spacings for the PA/G composites were 3.34, 2.02, and 1.67 Å for corresponding peaks at 26.6, 44.6, and 54.85°, respectively. This indicated the incorporation of graphite particles into the PA matrices.

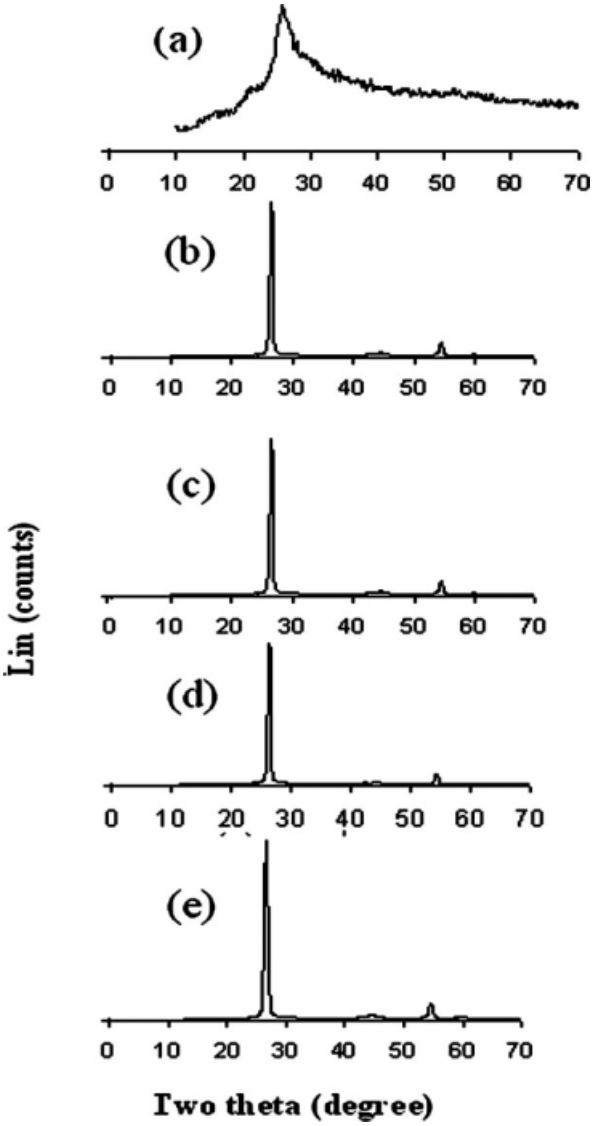

Figure 3 XRD of (a) PA powder, (b) graphite, (c) PA/G (0.2%), (d) PA/G (0.5%), and (e) PA/G (1.0%).

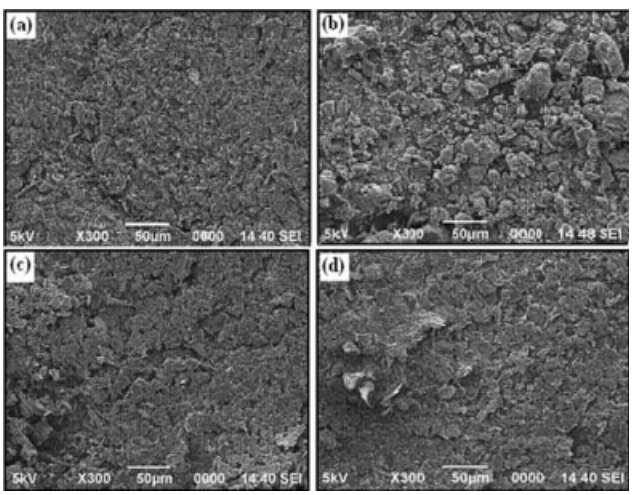

Figure 4 SEM micrographs of (a) graphite (20 μm), (b) PA, (c) PA/G (1.0%), and (d) PA/G (0.5%)

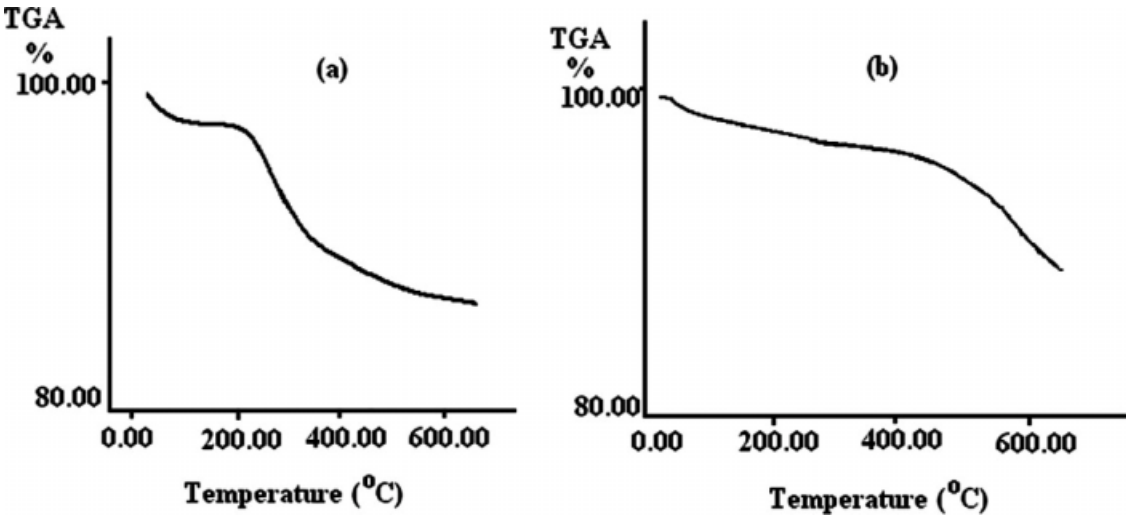

Figure 5 Thermogravimetric analysis (TGA) curves of the (a) PA and (b) PA/G composite.

Scanning electron microscopy (SEM)

The SEM images of the PA and PA/G composites are presented in Figure 4. In PA, the particles were randomly aggregated, and rough surfaces were observed, whereas the PA/G composites presented a surface with some holes and smooth regions. In the PA/G composites, the particles were bigger in size. This was possibly because of the adsorption of aniline hydrochloride on the surface of the graphite particles and subsequent polymerization. The PA/G composites showed a higher current, probably because of the rougher surface, as demonstrated by the SEM micrograph of the composites.[37]

Thermal analysis

The thermogravimetric profiles of the PA and PA/G composites (Fig. 5) showed similar patterns, with a small variation in the degradation temperature. The weight loss at 398 K revealed the loss of water molecules from the polymer matrix. The weight loss from 398 to 498 K was due to the removal of HCl bound to the PA chain and low-molecular-weight oligomers. The final degradation starting from 573 K was due to the degradation of the polymers.[38,39] The gradual weight loss over a wide range of temperature indicated the thermal stability of the PA/G composites.

Figure 6(a) shows the differential scanning calorimetry (DSC) curves for PA. This curve indicated an endothermic transition centered at 383 K. This endotherm could have been related to the evaporation of the water trapped inside the polymer or bonded to the polymer backbone. The processes was not believed to be a glass transition because, after the polymer was cooled and a second DSC was run, no exotherm transition was observed upon reheating.

In the DSC curve of the PA/G composite, two exothermic peaks were observed, as shown in Figure 6. With regard to the PA/G decomposition at 573 K,[40] the second broad and weak DSC peak at 584 K, shown in Figure 6(b), could have been due to such decomposition. Clearly, the decomposition temperature of PA in the PA/G composite was somewhat higher than that of pure PA. The difference in the thermal behavior may have arisen from a situation

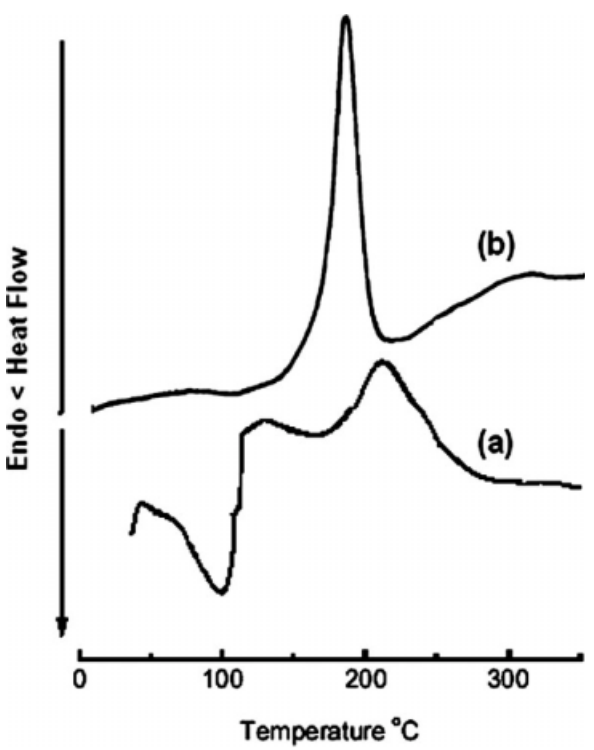

Figure 6 DSC curves of the (a) PA and (b) PA/G composite.

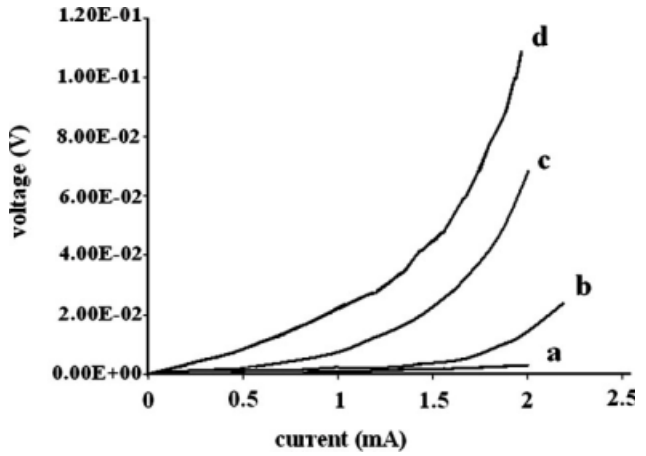

Figure 7 *I–V* curves of the (a) PA, (b) PA/G composite (0.2%), (c) PA/G composite (0.5%), and (d) PA/G composite (1.0%) investigated by the two-probe Keithley source meter.

in which PA intercalated into the graphite layers was very likely protected by the thin crumpled carbon sheets, which were formed from the graphite decomposition and then absorbed on PA surfaces; this prevented the decomposition of PA.

Direct-current (dc) conductivity

Figure 7 shows the *I–V* characteristic of PA and PA/G composites at room temperature. It was observed that *I–V* characteristic of PA was completely symmetrical with respect to *V*. The *I–V* characteristic of PA/G composites indicated that the PA/G composites behaved as Schottky junction.[16]

The conductivity of the PA and PA/G composites varied widely in the range 0.042–238.08 S/cm (Table I), depending on the various concentrations of the graphite added and the temperature increase. Figure 8 shows the variation of the conductivity of the polymer and composites with temperature. In PA, the conductivity first decreased with increasing temperature, which was caused by the removal of acid. PA showed maximum conductivity at 323 K (0.50 S/cm), but its conductivity was found in the same range, from 333 to 423 K. In the PA/G composite, the conductivity increased with increasing concentration of graphite. We incorporated graphite from 0.2 to 1.0% into the PA matrices, and the maximum conductivity (20.26 S/cm) was found in the 1.0% PA/G composite at room temperature. The increase in temperature resulted in a decrease in conductivity for the PA/G composites up to 313 K. The conductivity increased from 313 to 423 K, showing semiconducting behavior. The slight increase in temperature may have caused molecular and filler orientation instead of electron hopping from the highest occupied molecular orbital (HOMO) to the lowest unoccupied molecular orbital (LUMO) and, hence, caused the decreases in conductivity observed initially up to 313 K. The abrupt increase in conductivity for the PA/G composites with different compositions was also observed from 353 K. This may have been the result of increased intrachain and interchain hopping at high temperatures. An increase in interchain and intrachain hopping results in a high charge carrier mobility within the composite, which leads to an increase in the conductivity at appropriate high temperatures.[41]

TABLE I
Conductivity of the PA and PA/G Composites at Various Temperatures

Temperature (K)	Conductivity (S/cm)			
	PA	PA/G (0.2%)	PA/G (0.5%)	PA/G (1%)
300	0.044	3.77	15.45	20.26
308	0.042	2.56	10.07	12.45
313	0.042	3.61	10.07	13.86
323	0.050	4.53	10.57	13.86
333	0.044	5.37	13.61	18.30
353	0.046	5.65	16.86	30.22
373	0.046	40.21	122.54	143.50
423	0.046	56.72	198.01	238.08

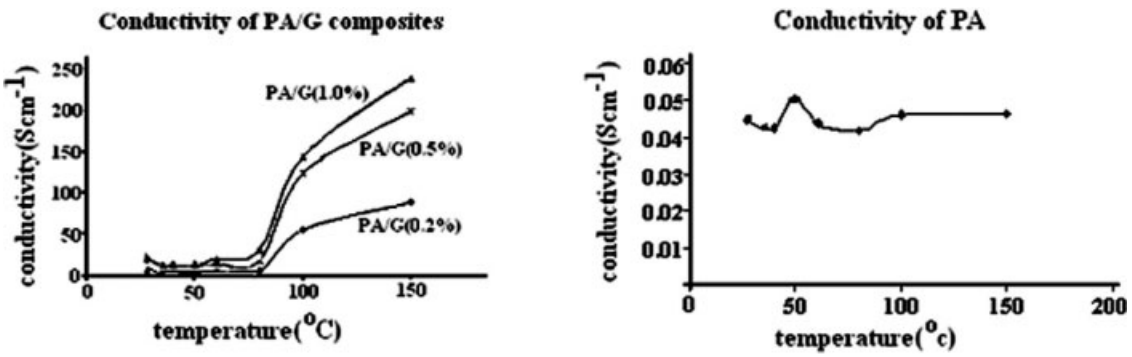

Figure 8 Conductivity of the PA/G composites and PA with respect to temperature.

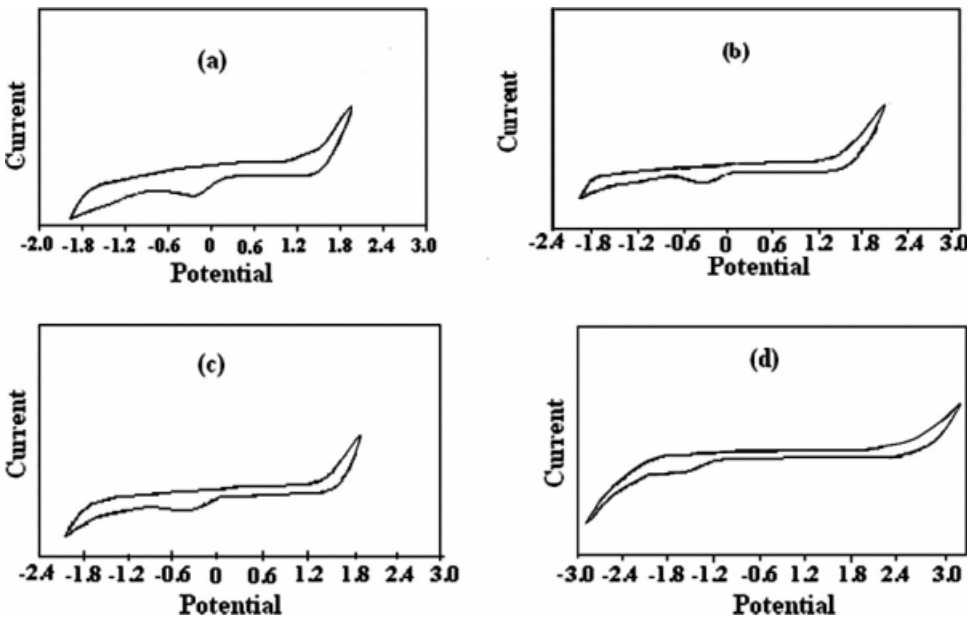

Figure 9 Cyclic voltammograms at different scan rates for (a) PA/G (1.0%), (b) PA/G (0.5%), (c) PA/G (0.2%), and (d) PA in a 1.0*M* HCl solution.

Electrochemical properties

PA/G films (0.2, 0.5, and 1.0%) on indium tin oxide coated glass, Ag/AgCl, and Pt wire were used as working electrodes, the reference electrode, and the counter electrode, respectively, with a 0.1*M* HCl solution as a supporting electrolyte prepared in 10 mL of acetonitrile. The PA/G composites were analyzed at a scan rate of 50 mV/s. Figure 9 shows the cyclic voltammogram of the PA and PA/G composites. The electrochemical band gap (E_g^{ec}) of the samples were calculated with the following formulas:[32]

$$\text{HOMO} = -[\varphi_{onset}^{ox} + 4.71](\text{eV}) \quad (2)$$

$$\text{LUMO} = -[\varphi_{onset}^{red} + 4.71](\text{eV}) \quad (3)$$

$$E_g^{ec} = (\varphi_{onset}^{ox} - \varphi_{onset}^{red})(\text{eV}) \quad (4)$$

where the units φ_{onset}^{ox} (onset oxidation potential) and φ_{onset}^{red} (onset reduction potential) are *V* versus Ag/AgCl. The values obtained are listed in Table II. The electrochemical band gap for PA was calculated from the voltammogram and was found to be 3.2 eV, whereas in the PA/G composites, the band gaps were found to decrease (from 1.6 to 1.2 eV) with increasing amounts of incorporated graphite. The incorporation of graphite resulted in a change in the electronic band structure, which manifested as new midgap state being created, and hence, a decrease in the band gap occurred.[42]

TABLE II
Electrochemical Data of the PA and PA/G Composites

Sample	$\phi_{onset}^{ox}/E_{HOMO}$	$\phi_{onset}^{red}/E_{LUMO}$	E_g^{ec} (eV)
PA	2.10/−6.81	−1.10/−3.61	3.2
PA/G composites			
0.2%	1.50/−6.21	−0.10/−4.61	1.6
0.5%	1.45/−6.16	−0.05/−4.66	1.5
1.0%	1.10/−5.81	−0.10/−4.61	1.2

E_{HOMO} and E_{LUMO} signify the highest occupied molecular orbital (HOMO) energy level and lowest unoccupied molecular orbital (LUMO) energy level respectively for the PA and PA/G composites.

Charge capacity

The area under the CV peaks was integrated to yield charge capacity, which in turn, provided information about the electroactivity of the PA/G composites. The CV study of the PA/G composite up to the 50th

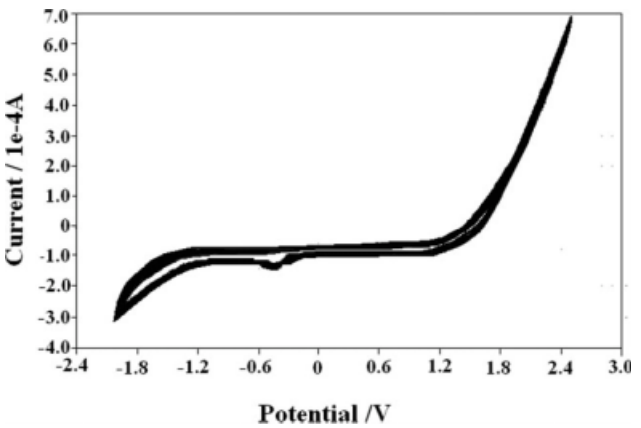

Figure 10 Successive electrochemical cycles for the PA/G (1.0%) composite up to the 50th cycle.

cycle revealed that the cathodic and anodic peaks were nearly symmetrical above each other with minimum separation. The charge capacity of the polymer composite did not diminish, even after repeated cycles (Fig. 10). This property emphasized that the PA/G composites may be useful and prominent materials for use in rechargeable batteries.

CONCLUSIONS

PA/G composites were successfully synthesized by the *in situ* polymerization of aniline in the dispersion of graphite in a 1.5*M* HCl solution. An SEM micrograph confirmed the uniform distribution of the graphite into the PA matrices. The thermal analysis revealed that the PA/G composites possessed good thermal stability up to 573 K. The band gap of the PA/G composites decreased to 1.2–1.6 eV compared to PA alone (3.2 eV) on addition of graphite (0.20–1.0%). The dc conductivity of the PA/G composites increased from 3.77 to 238.08 S/cm with increasing graphite and temperature as well, whereas the conductivity range for PA was 0.042–0.050 S/cm. The dc conductivity of the composites increased with temperature. However, in the initial stage of heating, the conductivity decreased because of the loss of solvent/trapped HCl. The PA/G composites showed gratifying reversible electrochemical response intake charge capacity, which was almost unchanged, even up to the 50th cycle.

References

1. Kanungo, M.; Kumar, A.; Contractor, A. Q. J Electroanal Chem 2002, 46, 528.
2. Lindfors, T.; Ivaska, A. Anal Chem Acta 2001, 171, 437.
3. Ivanov, A. N.; Lukachova, L.; Evtugyn, G. A.; Karyakina, E. E.; Kiseleva, S. G.; Budnikov, H. C.; Orlov, A. V.; Karpacheva, G. P.; Karyakin, A. A. Bio Anal Chem 2002, 55, 75.
4. Somani, P.; Mandel, A. B.; Radhakrishnan, S. R. Acta Mater 2000, 48, 2859.
5. Gurunathan, G.; Vadivel, M. A.; Marimuthu, P.; Mulik, U. P.; Amalnerkar, D. P. Mater Chem Phys 1999, 61, 173.
6. Rahmanifar, M. S.; Mousavi, M. F.; Shamsipur, M. J Power Sources 2002, 110, 229.
7. Rahmanifar, M. S.; Mousavi, M. F.; Shamsipur, M.; Ghaemi, M. J Power Sources 2004, 132, 296.
8. Karami, H.; Mousavi, M. F.; Shamsipur, M.; Riahi, S. J Power Sources 2006, 154, 298.
9. Banerjee, P.; Mandal, B. M. Synth Met 1995, 74, 257.
10. Hechavarría, L.; Hu, H.; Rincon, M. E. Thin Solid Films 2003, 441, 56.
11. Tsutsumi, H.; Yamashita, S.; Oishi, T. J Appl Electrochem 1997, 27, 477.
12. Neoh, K. G.; Pun, M. Y.; Kang, E. T.; Tan, K. L. Synth Met 1995, 73, 209.
13. Singla, M. L.; Awasthi, S.; Srivastava, A. Sens Actuators B 2007, 127, 580.
14. Zeng, X. R.; Ko, T. M. J Polym Sci Part B: Polym Phys 1997, 35, 1993.
15. Ghosh, P.; Sarkar, A.; Meikap, A. K.; Chattopadhyay, S. K.; Chatterjee, S. K.; Ghosh, M. J Phys D Appl Phys 2006, 39, 3047.
16. Dey, A.; De, S.; De, A.; De, S. K. Nanotechnology 2004, 15, 1277.
17. Somani, P.; Kale, B. B.; Amalnerkar, D. P. Synth Met 1999, 106, 53.
18. Fusalba, F.; Belanger, D. Electrochim Acta 2000, 45, 3877.
19. Somani, P. R.; Marimuthu, R.; Mandale, A. B. Polymer 2001, 42, 2991.
20. Himanshu, N.; Hailemichae, A.; Emmanue, I. Appl Mater Sci 2006, 203, 3665.
21. Wang, Z. H.; Scherr, E. M.; MacDiarmid, A. G.; Epstein, A. J Phys Rev B 1992, 45, 4190.
22. Mizoguchi, K.; Nechtschein, M.; Travers, J. P.; Menardo, C. Phys Rev Lett 1989, 63, 66.
23. Chen, G. H.; Wu, D. J.; Weng, W. G.; He, B.; Yan, W. I. Polym Int 2001, 50, 980.
24. Xu, J.; Hu, Y.; Song, L.; Wang, Q.; Fan, W. Mater Res Bull 2001, 36, 1833.
25. Raghu, A. V.; Lee, Y. R.; Jeong, H. M.; Shin, C. M. Macromol Chem Phys 2008, 209, 2487.
26. Lee, Y. R.; Raghu, A. V.; Jeong, H. M.; Kim, B. K. Macromol Chem Phys 2009, 210, 1247.
27. Pan, Q.; Wang, L.; Fang, S. Polym Adv Technol 2002, 14, 216.
28. Li, W.; Johnson, C. L.; Wang, H. L. Polymer 2004, 45, 4769.
29. Hu, J.; Xiao, S.; Zhong, L.; Zhu, H.; Gan, F. Mater Corros 2007, 58. 774.
30. Ghanbari, K.; Mousavi, M.; Shamsipur, M.; Karami, H. J Power Sources 2007, 170, 513.
31. Seredych, M.; Pietrzak, R.; Bandosz, T. J. Ind Eng Chem Res 2007, 46, 6925.
32. Bhadra, S.; Singha, N. K.; Khastgir, D. J Appl Polym Sci 2007, 104, 1900.
33. Stejskal, J.; Gilbert, R. G. Pure Appl Chem 2002, 74, 857.
34. Xiao, P.; Xiao, M.; Liu, P. G.; Gong, K. Carbon 2000, 38, 626.
35. Cao, Y.; Smith, P.; Heeger, A. J. Synth Met 1989, 32, 263.
36. Bredas, J. L.; Silbey, R. Conjugated Polymers; Kluwer: London, 1991.
37. Calixto, C. M. F.; Mendes, R. K.; Oliveira, A. C.; Ramos, L. A.; Cervini, P.; Cavalheiro, E. T. G. Mater Res 2007, 10, 109.
38. Deng, J. G.; He, C. L.; Peng, Y. X.; Wang, J. H.; Long, X. P.; Li, P. Synth Met 2003, 139, 295.
39. He, Y. J. Powder Technol 2004, 147, 59.
40. Sonobe, N.; Kyotani, T.; Tomita, A. Carbon 1990, 28, 483.
41. Leeuw, D. M.; Simenon, M. J.; Brown, A. R.; Einerhand, R. E. F. Synth Met 1997, 87, 53.
42. Skothein, T. A.; Elsenbaumer, R. L.; Reynolds, J. R. Handbook of Conducting Polymers, 2nd ed.; Marcel Dekker: New York, 1998.